# Vibrational spectra and structures of bare and Xe-tagged cationic $Si_nO_m^+$ clusters

Cite as: J. Chem. Phys. **141**, 104313 (2014); https://doi.org/10.1063/1.4894406
Submitted: 02 July 2014 • Accepted: 20 August 2014 • Published Online: 10 September 2014

**Marco Savoca, Judith Langer, Dan J. Harding, et al.**

# Vibrational spectra and structures of bare and Xe-tagged cationic $Si_nO_m^+$ clusters

Marco Savoca,[1] Judith Langer,[1] Dan J. Harding,[2] Dennis Palagin,[3] Karsten Reuter,[3] Otto Dopfer,[1,a)] and André Fielicke[1,a)]
[1]*Institut für Optik und Atomare Physik, Technische Universität Berlin, Hardenbergstr. 36, 10623 Berlin, Germany*
[2]*Institut für Physikalische Chemie, Georg-August-Universität Göttingen, Tammannstr. 6, 37077 Göttingen, Germany*
[3]*Lehrstuhl für Theoretische Chemie, Technische Universität München, Lichtenbergstr. 4, 85747 Garching, Germany*

(Received 2 July 2014; accepted 20 August 2014; published online 10 September 2014)

Vibrational spectra of Xe-tagged cationic silicon oxide clusters $Si_nO_m^+$ with n = 3–5 and m = n, n ± 1 in the gas phase are obtained by resonant infrared multiple photon dissociation (IRMPD) spectroscopy and density functional theory calculations. The $Si_nO_m^+$ clusters are produced in a laser vaporization ion source and Xe complexes are formed after thermalization to 100 K. The clusters are subsequently irradiated with tunable light from an IR free electron laser and changes in the mass distribution yield size-specific IR spectra. The measured IRMPD spectra are compared to calculated linear IR absorption spectra leading to structural assignments. For several clusters, Xe complexation alters the energetic order of the $Si_nO_m^+$ isomers. Common structural motifs include the $Si_2O_2$ rhombus, the $Si_3O_2$ pentagon, and the $Si_3O_3$ hexagon. © *2014 AIP Publishing LLC*. [http://dx.doi.org/10.1063/1.4894406]

## I. INTRODUCTION

One of the key aims of nanoscience and cluster research is the development of new materials with novel tailored properties using nanoparticles as building blocks.[1] Recent efforts have led to the development of new techniques for the modification of nanoparticle properties such as doping,[2–5] functionalization,[6,7] surface modification,[7] or hybrid formation.[8] The electronic structure of small clusters also depends significantly on their size.[9] Silicon plays a major role as one of the technologically most important materials. The detection of luminescence in porous silicon[10] opened up new fields of application for silicon nanoparticles. For instance, Si nanocrystals in wide-gap dielectric matrices[11] provide efficient light emission in the near IR and visible spectral range. Unfortunately, bare silicon clusters are highly reactive due to their electronic configuration and dangling bonds. Hydrogen termination is an effective means of passivation and stabilization of silicon clusters.[12–17] There is also significant interest in $SiO_2$ matrices with embedded nanocrystalline silicon.[18–20] For small isolated $Si_n$ clusters, dissociative adsorption of dioxygen molecules has a significant impact on their geometry and electronic structure.[21] For silicon monoxide clusters $(SiO)_n$, two different structural types were proposed, namely, the so-called "silicon cored" structures with $sp^3$ silicon cores inside a silicon oxide shell[22,23] and the "silicon segregated" structures consisting of a bipyramidal silicon cluster attached to a stable $Si_nO_m$ subunit.[24] The HOMO-LUMO gap of the $Si_nO_m$ clusters tends to increase with increasing amount of oxygen.[25,26]

Silicates, a subset of silicon oxide nanoparticles, are important constituents of circumstellar and interstellar media. Since SiO is the dominant oxygen-bearing species in molecular astronomy, it has been proposed as a precursor to silicate formation via clustering of SiO molecules,[22,27,28] but the detailed formation process is still far from being understood. Silicates containing Si–Si bonds are also currently believed to be candidates for the observed extended red emission in the diffuse galactic background.[29,30]

Despite the importance of silicon oxides, only limited spectroscopic studies of their clusters are available. Several $Si_nO_m^-$ species have been characterized by anion photoelectron spectroscopy,[31–34] while neutral silicon monoxide clusters have been studied by infrared (IR) and Raman spectroscopy in rare gas matrices.[35–37] The most recent spectroscopic data are from infrared multiple photon dissociation (IRMPD) of stoichiometric silicon monoxide cluster cations, $(SiO)_n^+$ with n = 3–5, by Garand *et al.*[38] monitoring the loss of SiO. The spectra were compared to linear IR absorption spectra from density functional theory (DFT) calculations. The IR spectra of n = 3 and 5 were assigned to a single isomer, whereas for n = 4 the presence of two isomers was suggested and rationalized by incomplete thermal equilibration. As will be shown below, the calculated lowest energy structures are consistent with those reported here.

Here, we report gas-phase IRMPD spectra for silicon oxide cluster cations with stoichiometric $(SiO)_n^+$ and non-stoichiometric composition for n = 3–5. In comparison to the earlier measurements,[38] spectra of cold clusters are obtained in an extended spectral range using Xe atoms as messengers. This messenger technique is a variant of action spectroscopy where mass spectrometrically detectable processes,

a)Authors to whom correspondence should be addressed. Electronic addresses: dopfer@physik.tu-berlin.de and fielicke@physik.tu-berlin.de

 

here the evaporation of weakly bound Xe ligands, are used to probe the absorption of photons.[39,40] The binding of rare gas atoms assures the presence of a cold complex and largely reduces the dissociation energy. Often, for strongly bound clusters it is justified to assume that the impact of the messenger on the intrinsic properties of the bare cluster is negligible, and therefore the IR spectra are not significantly affected by the presence of the messenger. Nevertheless, in some cases a greater influence on the energetic, structural, vibrational, and electronic properties has been reported.[41–45] The magnitude of these perturbation effects usually depends on the polarizability of the rare gas atom. Therefore, the lighter rare gases are often used in an attempt to minimize the perturbations, but in our case xenon had to be used because complexes with lighter rare-gas ligands were not formed in the employed cluster ion source. Xenon also has the lowest ionization energy of all rare gases, and it will be shown that partial electron transfer from Xe toward the silicon oxide cluster leads to additional stabilization of the Xe complexes. A detailed analysis of the influence of the Xe messenger on the $Si_nO_m^+$ clusters is not the main goal of this work, but will be discussed for species where the Xe binding has a significant effect.

## II. METHODS

### A. Experimental

The experiments have been performed in a molecular beam setup located at a beam line of the Free Electron Laser for Infrared eXperiments (FELIX).[46] Details of the experimental setup and procedure have been reported previously.[47,48] Briefly, silicon atoms and clusters are generated by laser ablation from a Si rod using the second harmonic (532 nm) output of a Nd:YAG laser operating at 20 Hz. The plume is then crossed with a short gas pulse consisting of a mixture of 0.01% $O_2$ and 0.5% $^{129}$Xe in He. $Si_nO_m^+$–Xe complexes are formed within a copper expansion channel held at ∼100 K by cooling with liquid nitrogen. The resulting molecular beam is first skimmed and then shaped through a 1 mm aperture before entering the extraction region of a time-of-flight mass spectrometer to analyze the mass distribution of the cationic complexes. IRMPD of these species is achieved by overlapping the molecular beam with the intense IR light from FELIX operating at 10 Hz. IRMPD spectra are derived from measuring the variation of the cluster mass distribution induced by resonant absorption of IR photons. The resulting evaporation of one or more $^{129}$Xe atoms as a function of the irradiating IR frequency is monitored in the 250–1250 $cm^{-1}$ range. The reported IRMPD spectra are obtained by converting the mass specific depletion to an absorption cross-section $\sigma(\nu)$ with subsequent normalization by the IR photon flux, $\sigma(\nu) = \ln(I_{off}/I_{on}(\nu))/\Phi(\nu)$, where $I_{on}$ and $I_{off}$ are the ion signal intensities with and without IR light, respectively.

### B. Computational

In an initial step, candidate structures of $Si_nO_m^+$ clusters were explored using DFT-based basin hopping global optimization.[49] The calculations were performed using the FHI-aims package[50] with the PBE functional[51] and tier 2 numerical basis sets. This search provided a general overview of the geometric and energetic properties of the bare silicon oxide clusters. Due to the apparent influence of the Xe messenger atom on the properties of the complexes, additional calculations were also performed with explicit inclusion of the Xe atom(s). To this end, a basin hopping global optimization algorithm[52] has been used together with the TURBOMOLE V6.3.1 program package.[53] The initial structure search was conducted at the RI-BP86/def2-SVP level of theory.[54,55] The final optimization and calculation of vibrational spectra was performed using the Tao-Perdew-Staroverov-Scuseria (TPSS) functional[56] along with the def2-TZVP basis set,[57,58] the corresponding effective core potential (ECP) for Xe, and the resolution-of-identity (RI) approximation.[59] This approach has been used in our previous work on $Si_4Xe^+$,[41] where it properly described the substantial Si–Xe interaction. Initial test calculations for $Si_3O_2^+$ with increasing basis set size suggest that the def2-TZVP basis set is well-balanced in terms of resulting quality and computational effort. All identified low-energy isomers have a doublet electronic ground state. Relative energies include zero-point vibrational energies. Harmonic vibrational frequencies are scaled by a factor of 1.025, obtained by comparison of the calculated Si–O stretching frequencies with those measured for SiO[60] and $SiOH^+$.[61] Finally, the theoretical IR stick spectra are convoluted with a Gaussian line profile adopting a full width at half-maximum of 10 $cm^{-1}$.

## III. RESULTS AND DISCUSSION

In the following, we compare the experimental IRMPD spectra of the Xe-tagged $Si_nO_m^+$ clusters to IR spectra predicted for the respective lowest energy isomers of bare $Si_nO_m^+$ and—if required—relevant higher energy isomers (Figs. 1–3). A comparison to the corresponding Xe complexes is carried out for the lowest energy isomers and, if this does not allow for a conclusive assignment, also for higher energy isomers. The latter become particularly relevant in cases where the energetic order of the $Si_nO_m^+$ isomers is altered by Xe complexation.

The most intense modes in the IRMPD spectra are observed in the frequency range from 400 to 1200 $cm^{-1}$ and correspond to Si–O stretching vibrations ($\sigma_{SiO}$). The Si–Si stretching vibrations ($\sigma_{SiSi}$) and the deformation modes have typically lower frequencies and significantly lower IR intensity. Relevant vibrational and structural data of all clusters investigated along with the vibrational and isomer assignments of the experimental bands are given in Figs. S1–S16 and Tables T1–T5 in the supplementary material.[71] The widths of the bands in the IRMPD spectra are typically a few tens of $cm^{-1}$. Thus, the accuracy of the reported band positions is of the order of ±5 $cm^{-1}$.

### A. $Si_3O_m^+$(–Xe), m = 2–4

#### 1. $Si_3O_2^+$(–Xe)

The IR spectra for this cluster size are depicted in the left panel of Fig. 1. The IRMPD spectrum for $Si_3O_2^+$–Xe shows

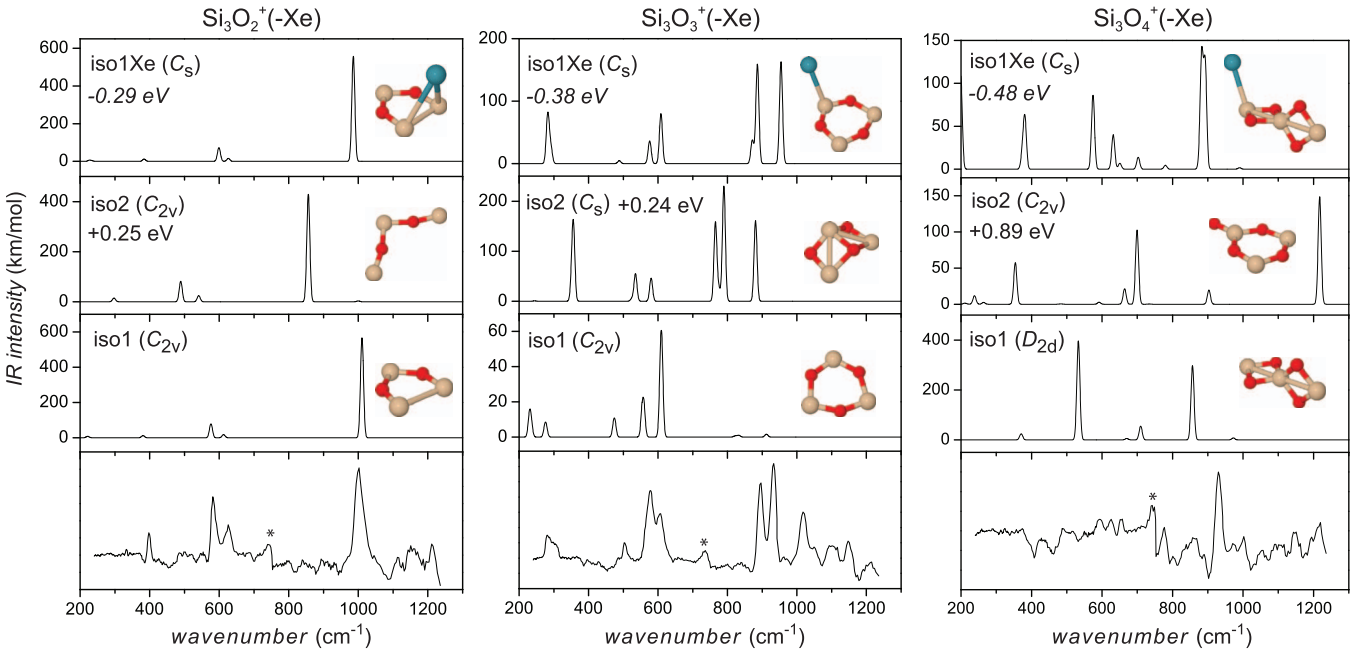


FIG. 1. IRMPD spectra of $Si_3O_m^+$–Xe (m = 2–4) compared to linear IR absorption spectra calculated for relevant $Si_3O_m^+$(–Xe) isomers. The symmetry group is given in parenthesis. Relative energies and Xe binding energies (italic) are given in eV. The experimental spectra were recorded in smaller sections (150–200 $cm^{-1}$ each), and the asterisk marks the switchover between two of these sections, where the signal base line drops to a lower level, due to slight changes in the experimental conditions. Further structures and IR spectra calculated for $Si_3O_m^+$(–Xe) are available in Figs. S1–S6 in the supplementary material.[71]

distinct bands at 398, 582, 626, and 1002 $cm^{-1}$. The overall match with the spectrum predicted for the lowest energy $Si_3O_2^+$ isomer (iso1) is good, and the four measured bands are assigned to the four transitions calculated at 381, 576, 613, and 1011 $cm^{-1}$ (Table T1 in the supplementary material).[71] The small maximum and average deviations of 17 and 11 $cm^{-1}$ indicate that Xe tagging has only a minor impact on the IR spectrum. Iso1 is a planar pentagon with $C_{2v}$ symmetry and has been found as most stable structure in previous DFT calculations at the B3LYP/6-31G+(d) level.[62] Xe complexation of iso1 reduces the symmetry from $C_{2v}$ to $C_s$, as Xe is bridging the Si–Si bond out of the plane of the ring. The Si–Xe bond length is 3.34 Å, and the binding energy amounts to −0.29 eV (−27.72 kJ/mol). The Si–Si bond contracts from 2.84 to 2.72 Å upon Xe complexation. Inspection of Fig. 1 and Table T1 confirms that the IR spectrum of iso1–Xe is indeed essentially the same as that of the bare ion.

The next higher energy isomer, iso2 (+0.25 eV), has a planar open triangular structure ($C_{2v}$ symmetry) and can be derived from iso1 by breaking the Si–Si bond. Its IR spectrum is very different from the measured IRMPD spectrum, and the most intense band predicted at 856 $cm^{-1}$ clearly has no visible counterpart. This anti-symmetric Si–O stretching vibration (853 $cm^{-1}$, $b_1$) has essentially no IR activity for iso1. In addition, the symmetric Si–O stretch of iso2 predicted at 999 $cm^{-1}$ is roughly 140 times weaker than the corresponding mode for iso1 at 1011 $cm^{-1}$ (566 km/mol, $a_1$). IR spectra of higher-energy isomers and their Xe complexes presented in Figs. S1 and S2 in the supplementary material[71] do not agree with the measured IRMPD spectrum.

According to our calculations, the main difference between the geometric structure of $Si_3O_2^+$ (iso1) and that of the most stable neutral isomer, a similar pentagon ($C_{2v}$) in a $^3B_1$ state,[33,63,64] is an elongation of the Si–Si bond by around 0.4 Å. Other bond lengths in the cluster change little upon ionization. Indeed, the ground state structure of neutral $Si_3O_2$ is unclear because other calculations predict a pyramidal global minimum with a singlet electronic ground state.[26,65]

### 2. $Si_3O_3^+$(–Xe)

The IR spectra of $Si_3O_3^+$(–Xe) are presented in the middle panel of Fig. 1. The IRMPD spectrum of $Si_3O_3^+$–Xe features prominent peaks at 282, 502, 578, 608, 896, and 933 $cm^{-1}$, and a few more bands above 1000 $cm^{-1}$. The spectrum calculated for iso1, a planar $Si_3O_3^+$ hexagon, provides a relatively good match to the experiment in the low frequency range (250–650 $cm^{-1}$) but dramatically underestimates the intensities of the bands observed at higher wavenumber, namely, the three very weak bands predicted at 823, 833, and 912 $cm^{-1}$ (Table T1 in the supplementary material).[71] This discrepancy is resolved when the Xe ligand is explicitly included in the calculations, because the three corresponding $\sigma_{SiO}$ bands of iso1-Xe at 872, 886, and 954 $cm^{-1}$ gain drastically in IR intensities upon Xe complexation by roughly two orders of magnitude. As a consequence, the spectrum calculated for iso1-Xe provides a good match to the experimental spectrum with respect to both the vibrational frequencies and the IR intensities.

The large change in the spectrum of iso1 induced by complexation with Xe can be related to its structural properties. The six-membered ring structure of $Si_3O_3^+$ with alternating Si–O bonds ($C_{2v}$) is similar to the predicted neutral ground state with $D_{3h}$ symmetry.[26,33,38,62,64–68] The cation

experiences either dynamic or static Jahn-Teller distortion to $C_{2v}$ symmetry,[38] so that the frequencies and IR intensities of the calculated transitions strongly depend on the degree of distortion from $D_{3h}$ to $C_{2v}$. The Jahn-Teller effect is eliminated by the complexation with Xe, which causes a further symmetry reduction to $C_s$ in the $Si_3O_3^+$–Xe complex. This may explain why the overall match between the IRMPD spectrum and that predicted for iso1-Xe is significantly better than that predicted for the bare $Si_3O_3^+$ ion (iso1). The Xe atom in iso1-Xe binds out-of-plane to the Si atom at the apex of the planar ring at a distance of 2.95 Å with a binding energy of −0.38 eV (−36.63 kJ/mol). This is the same binding site as for the protonation.[62]

We also observe additional bands between 1000 and 1200 $cm^{-1}$ in the IRMPD spectrum that are not reproduced by the calculations. They are tentatively attributed to combination bands and overtones. The peak at 1018 $cm^{-1}$ could be the first overtone of the mode at 502 $cm^{-1}$, and the peak at 1147 $cm^{-1}$ could be the combination of the 578 and 608 $cm^{-1}$ modes. Contributions from other high energy isomers to the IRMPD spectrum can be excluded. The second lowest isomer, iso2 (+0.24 eV), has a very different spectrum. The only isomer with an intense band predicted above 1100 $cm^{-1}$ is iso3 (+0.39 eV, Fig. S3 in the supplementary material),[71] but its spectrum does not match in the remaining spectral range. For similar reasons, iso5 (+1.69 eV, Fig. S3 in the supplementary material)[71] with an intense transition at 1028 $cm^{-1}$ can be excluded. In contrast to iso1, Xe complexation to these higher energy isomers does not change the appearance of their IR spectra.

Interestingly, the experimental IRMPD spectrum of $Si_3O_3^+$–Xe shows overall good agreement with the corresponding spectrum for the bare $Si_3O_3^+$ ion reported by Garand *et al.*,[38] although the calculated spectra for $Si_3O_3^+$–Xe and $Si_3O_3^+$ differ significantly. Nevertheless, closer inspection reveals notable differences in the width, position, and relative intensity of the transitions. For example, the prominent band observed at 1080 $cm^{-1}$ in the $Si_3O_3^+$ spectrum (labeled band C) does not appear as single intense band in the $Si_3O_3^+$–Xe spectrum.

#### 3. $Si_3O_4^+$(–Xe)

The IRMPD spectrum of $Si_3O_4^+$–Xe (right panel in Fig. 1) displays low signal to noise ratio, and only a single peak at 930 $cm^{-1}$ can clearly be identified. The calculated lowest energy $Si_3O_4^+$ isomer, iso1 ($D_{2d}$), consists of two rhombic $Si_2O_2$ units with two bridging oxygen atoms, which are fused together in a perpendicular configuration such that a linear Si–Si–Si chain is formed, with the central Si atom being tetrahedrally coordinated to four O atoms. This structure corresponds also to the lowest energy isomer of neutral $Si_3O_4$.[11,32,67] The Xe atom in iso1-Xe ($C_s$) binds to a terminal silicon atoms in the symmetry plane at a distance of 2.89 Å, with a bond energy of −0.48 eV (−46.21 kJ/mol). As for $Si_3O_3^+$, the spectrum calculated for iso1-Xe fits the experimental one better than that of bare iso1. The observed band is assigned to an unresolved doublet predicted at 883 and 893 $cm^{-1}$, which are anti-symmetric $\sigma_{SiO}$ vibrations in the Xe–$Si_2O_2$ and $Si_2O_2$ units, respectively. These two transitions arise from a splitting of the doubly degenerate vibration of bare iso1 at 857 $cm^{-1}$ due to symmetry reduction from $D_{2d}$ to $C_s$ upon Xe complexation.

The energetically closest isomer, iso2 ($C_{2v}$, +0.89 eV), lies very high in energy and consists of a planar cyclic $Si_3O_3$ unit with an additional dangling Si–O bond in the molecular plane. Its predicted IR spectrum is quite different from the measured IRMPD spectrum. Similar conclusions apply to the IR spectra of other higher-energy isomers and their Xe complexes presented in Figs. S5 and S6 in the supplementary material.[71]

### B. $Si_4O_m^+$(–Xe), m = 3–5

#### 1. $Si_4O_3^+$(–Xe)

The IR spectra of this cluster species are shown in the left panel of Fig. 2. The IRMPD spectrum of $Si_4O_3^+$–Xe exhibits prominent bands at 534, 872, and 1077 $cm^{-1}$. The calculations for bare $Si_4O_3^+$ yield two nearly degenerate lowest energy isomers, iso1 ($C_1$) and iso2 ($C_1$), which are separated by only 0.03 eV. Iso1 has a non-planar structure with a five-membered $Si_3O_2$ ring fused to a $Si_2O_2$ rhombus. Iso2 is an asymmetric seven-membered ring with one Si–Si and three Si–O–Si units. Indeed, only the spectrum calculated for iso2 agrees with the IRMPD spectrum. For instance, the intense peak observed at 1077 $cm^{-1}$ is only reproduced in the iso2 spectrum. The three transitions in the IRMPD spectrum are then assigned to the $\sigma_{SiO}$ vibrations of iso2 calculated at 515, 880, and 1061/1064 $cm^{-1}$, respectively (Table T2 in the supplementary material).[71] The iso1 isomer is not observed because its binding energy to Xe is significantly lower than that of iso2 (−0.29 vs. −0.22 eV). For both iso1 and iso2, Xe complexation has only a minor impact on the appearance of their IR spectra. In iso2-Xe, the Xe binds to one atom of the Si–Si pair at a distance of 3.14 Å.

Interestingly, the energetic order of the bare $Si_4O_3^+$ isomers is drastically changed by Xe complexation (see Figs. S7 and S8 in the supplementary material[71] for iso1-iso6). The predicted lowest energy complex, iso6-Xe, has a relatively high-energy $Si_4O_3^+$ core, and the next isomer in the energetic order is the observed iso2-Xe complex (+0.11 eV). Iso6 of $Si_4O_3^+$ ($C_{2v}$, +0.24 eV) is a six-membered ring, like the most stable $Si_3O_3^+$ isomer, but has the additional Si atom bound to one Si in the ring. In iso6-Xe, the Xe binds at a distance of 2.86 Å to the dangling Si atom in a right angle with the Si–Si pair with a binding energy of −0.54 eV (−52.29 kJ/mol). Thus, the binding energy iso6-Xe is more than twice the one of iso2-Xe (−0.22 eV, −21.08 kJ/mol). The complexation is in both cases accompanied by a transfer of electron density from Xe to the $Si_4O_3^+$ cluster. According to a natural population analysis,[69] the partial charge of the binding Si decreases from 0.54 to 0.28 e for iso6 and from 1.09 to 0.96 e for iso2, while the Xe atoms have charges of 0.27 and 0.16 e, respectively. The larger stabilization of iso6-Xe is rationalized by the larger charge transfer, leading to a stronger and shorter Si–Xe bond (3.14 vs. 2.86 Å). As the IR spectrum predicted for iso6-Xe does not match the observed IRMPD spectrum, we conclude that bare iso6

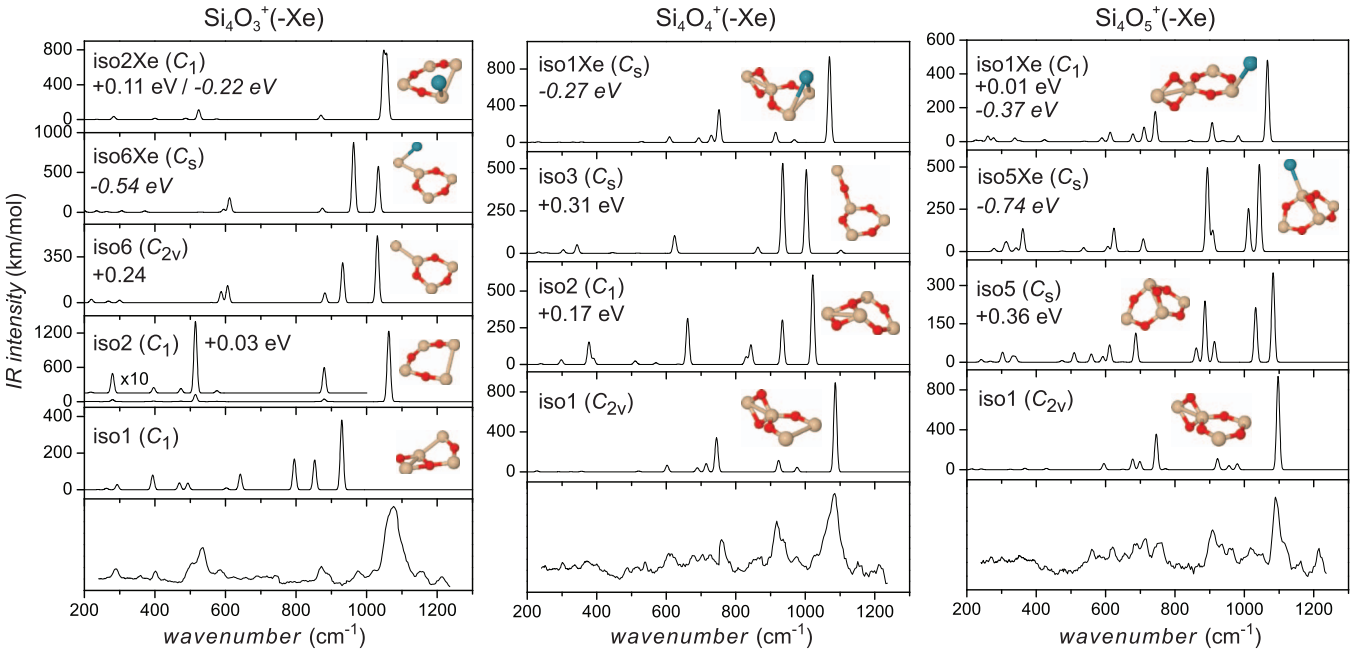


FIG. 2. IRMPD spectra of $Si_4O_m^+$–Xe (m = 3–5) compared to linear IR absorption spectra calculated for relevant $Si_4O_m^+$(–Xe) isomers. The symmetry group is given in parenthesis. Relative energies and Xe binding energies (italic) are given in eV. Further structures and IR spectra calculated for $Si_4O_n^+$(–Xe) are available in Figs. S7–S12 in the supplementary material.[71]

is not present in the $Si_4O_3^+$ population. Thus, in contrast to iso2-Xe, iso6-Xe cannot be formed, although it is the most stable $Si_4O_3^+$–Xe isomer, indicating that $Si_4O_3^+$ does not isomerize upon Xe complexation. Similar to iso1-Xe and iso6-Xe, also the IR spectra predicted for the other $Si_4O_3^+$–Xe isomers are not compatible with the measured IRMPD spectrum (Fig. S8 in the supplementary material).[71]

For neutral $Si_4O_3$ clusters different structures are found. DFT calculations at the B3LYP/6-31G(d)[26] and BP86/TZP[65] levels predict the lowest energy isomer to correspond to iso5 of the cation (+0.16 eV), and iso1 of $Si_4O_3^+$ corresponds to the third lowest isomer of neutral $Si_4O_3$.[26]

### 2. $Si_4O_4^+$(–Xe)

The IR spectrum measured for $Si_4O_4^+$–Xe is depicted in the middle panel of Fig. 2 and shows three distinct bands at 759, 918, and 1085 $cm^{-1}$, which can readily be assigned to $\sigma_{SiO}$ vibrations of iso1 calculated at 745, 923, and 1086 $cm^{-1}$. The effect of the Xe atom on the appearance of the IR spectrum of iso1 is negligible, with shifts of less than 17 $cm^{-1}$ for the three intense transitions. Iso1 ($C_{2v}$) consists of a planar $Si_3O_2$ pentagon joined at 90° to a planar $Si_2O_2$ rhombus. Their common Si atom is tetrahedrally coordinated by four O atoms. The $Si_3O_2$ unit is structurally very similar to iso1 of $Si_3O_2^+$, with Si–Si bond lengths of 2.89 Å. This example shows that smaller clusters can act as building blocks for larger ones without significant restructuring. Iso2 (+0.17 eV, $C_1$) is similar to iso1 of $Si_4O_3^+$ but with the additional O atom inserted into a Si–Si bond. It is composed of a distorted $Si_3O_3$ hexagon and a rhombic $Si_2O_2$ unit. Iso3 (+0.31 eV, $C_s$) consists of a $Si_3O_3$ ring attached to a nearly linear Si–O–Si chain with a Si–O–Si angle of 169.9°.

In contrast to $Si_4O_3^+$, Xe has no impact on the order of the three lowest energy isomers of $Si_4O_4^+$. Xe binds to iso1 via both Si atoms of the Si–Si pair, as in the case of $Si_3O_2^+$, and reduces the symmetry from $C_{2v}$ to $C_s$. The Si–Si bond length in the $Si_3O_2$ unit shrinks from 2.89 to 2.77 Å upon Xe complexation. The Xe binds in the $Si_2O_2$ plane with −0.27 eV (−26.45 kJ/mol) to the Si atoms at a distance of 3.36 Å. This binding motif is the same as for iso1-Xe of $Si_3O_2^+$ (−0.29 eV, −27.72 kJ/mol, 3.05 Å). Interestingly, a less stable iso1-Xe′ isomer with a different Xe binding site (at the $Si_2O_2$ rhombus) has a spectrum similar to that of iso1-Xe and may thus also contribute to the measured IRMPD spectrum. Based on their Xe binding energies (−0.06 vs. −0.27 eV), the iso1-Xe′ population is probably minor. The IR spectra predicted for higher energy $Si_4O_4^+$(–Xe) isomers available in Figs. S9 and S10 in the supplementary material[71] differ for all isomers within 0.5 eV of iso1 substantially from the measured IRMPD spectrum.

The IRMPD spectrum of untagged $Si_4O_4^+$ reported before[38] is significantly different from that of $Si_4O_4^+$–Xe shown in Fig. 2. For example, the former does not exhibit the intense peak at 1085 $cm^{-1}$ and the overall spectrum does not compare well to the spectrum calculated for iso1. Therefore, it was concluded that both iso1 and iso2 contribute to the IRMPD spectrum of $Si_4O_4^+$ recorded at ∼70 K. In contrast, the IRMPD spectrum of $Si_4O_4^+$–Xe recorded at similar temperature (∼100 K) is well reproduced by only a single isomer, namely that of the iso1, and there is no indication for the presence of iso2. As the calculated Xe binding energies are similar for both iso1 and iso2 (−0.27 and −0.16 eV), Xe complexation should not significantly change the population ratio of both $Si_4O_4^+$ isomers. At present, the reason for the very different appearance of the IRMPD spectra of $Si_4O_4^+$

and $Si_4O_4^+$–Xe is unclear. It may be related to the large difference in the dissociation energies of both systems (for loss of SiO and Xe, respectively), which require a very different number of IR photons to be absorbed for inducing IRMPD. Thus, the strongly nonlinear IRMPD process may perturb the IR spectrum of the bare ion much more severely than for the Xe-tagged species. According to our calculations the dissociation energy for the loss of SiO is 2.57 eV (247.92 kJ/mol, 2.55 eV in Garand *et al.*[38]). Therefore, around 20 IR photons with 1000 $cm^{-1}$ (0.12 eV) are required for fragmentation, in contrast to the approximately 2 photons required for Xe evaporation.

The predicted lowest energy structure of neutral $Si_4O_4$ corresponds to iso4 of the cation (+0.38 eV).[23,26,62,65–68,70]

### 3. $Si_4O_5^+$(–Xe)

The IRMPD spectrum of $Si_4O_5^+$–Xe in the right panel of Fig. 2 shows two distinct features at 909 and 1084 $cm^{-1}$. It closely resembles the spectra predicted for iso1 and iso1-Xe of $Si_4O_5^+$. These two intense bands are assigned to $\sigma_{SiO}$ vibrations predicted at 923 and 1097 $cm^{-1}$ (907 and 1066 $cm^{-1}$) for iso1 (iso1-Xe). Further weaker bands in the IRMPD spectrum are observed between 550 and 800 $cm^{-1}$. Indeed, several bands are predicted in this spectral range for iso1 and iso1-Xe, but we refrain from a detailed assignment due to the low signal-to-noise ratio. Iso1 ($C_{2v}$) is similar to the most stable structure of $Si_4O_4^+$ and consists of a $Si_2O_2$ and a $Si_3O_3$ building block. These two units are fused under 90° and share one Si atom that is tetrahedrally coordinated by four O atoms. The Xe atom binds to iso1 to a Si atom at one side of the $Si_3O_3$ unit at a distance of 2.95 Å with a binding energy of −0.37 eV (−35.76 kJ/mol).

Xe complexation has again a big impact on the energetic order of the $Si_4O_5^+$ clusters. Indeed, iso5-Xe is predicted to be the most stable $Si_4O_5^+$–Xe isomer, although bare iso5 is 0.36 eV higher in energy than iso1. The butterfly structure of iso5 ($C_s$) consists of two $Si_3O_2$ units with a shared Si–Si bond, which is bridged by an additional O atom. The Xe atom binds to iso5 at a relatively short distance of 2.71 Å to one of the Si atoms of the Si–O–Si bridge, with an exceptionally high binding energy of −0.74 eV (−71.65 kJ/mol), and is located in the symmetry plane spanned by the Si–O–Si bridge. This binding energy represents the upper limit of all Xe binding energies found in the current study. This high Xe binding energy arises from the high degree of electron transfer of 0.36 e from Xe to $Si_4O_5^+$. For comparison, the electron transfer in iso1-Xe amounts only to 0.24 e leading to a much weaker bond to Xe. As a consequence, iso5-Xe is predicted to be the ground state of $Si_4O_5^+$–Xe, which is however essentially isoenergetic with iso1-Xe (+0.01 eV). Closer inspection of Fig. 2 in the frequency region 900–1100 $cm^{-1}$ reveals that indeed a modest contribution of iso5-Xe to the measured IRMPD spectrum cannot be completely ruled out. The IR spectra predicted for other $Si_4O_5^+$(–Xe) isomers compared in Figs. S11 and S12 in the supplementary material[71] differ more substantially from the experimental IRMPD spectrum.

The structure identified for the $Si_4O_5^+$ cation is similar to the ground state structure predicted for the neutral cluster.[26,65,67] A neutral isomer corresponding to iso5 is calculated to be more than 4 eV above the most stable one.[26]

## C. $Si_5O_m^+$(–Xe), m = 4–6

### 1. $Si_5O_4^+$(–Xe)

The IR spectra of $Si_5O_4^+$ are presented in the left panel of Fig. 3, and the IRMPD spectrum of $Si_5O_4^+$–Xe exhibits

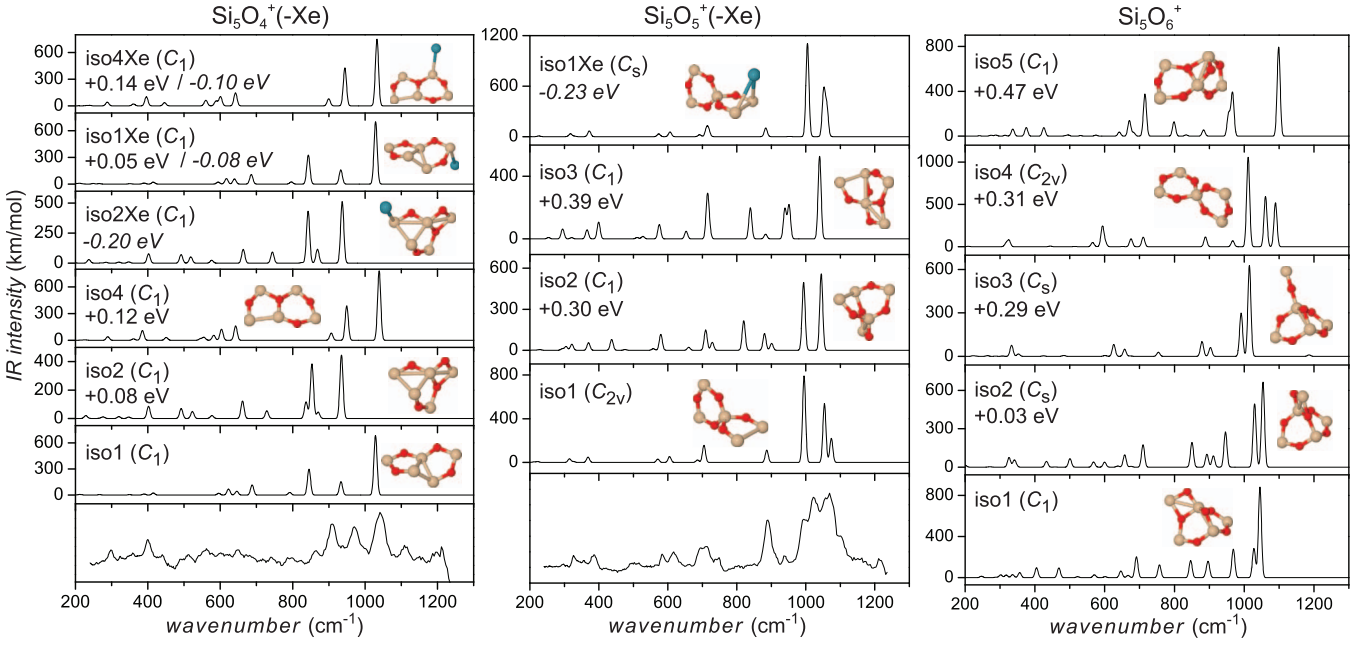


FIG. 3. IRMPD spectra of $Si_5O_m^+$–Xe (m = 4–5) compared to linear IR absorption spectra calculated for relevant $Si_5O_m^+$(–Xe) isomers. For $Si_5O_6^+$ only calculated IR spectra for five isomers up to 0.5 eV are shown. The symmetry group is given in parenthesis. Relative energies and Xe binding energies (italic) are given in eV. Further structures and IR spectra calculated for $Si_5O_m^+$(–Xe) are available in Figs. S13–S16 in the supplementary material.[71]

features at 298, 400, 909, 970, and 1041 $cm^{-1}$. Notably, four $Si_5O_4^+$ isomers are predicted within 0.12 eV above the most stable one, and the assignment is less clear than for the other cluster sizes. The best agreement is found with the spectrum of the fourth isomer in the energetic order, iso4 (+0.12 eV), although the spectrum of iso1 appears very similar. Nevertheless, the overall match is better for iso4, especially for the peak positions of the three features between 900 and 1050 $cm^{-1}$, which fit less well for iso1. The differences between iso4 and iso4–Xe are very small. Iso2 and iso3 alone cannot account for the observed spectrum.

The suggested isomer iso4 ($C_1$) is nearly planar and consists of a $Si_3O_2$ ring fused to a $Si_3O_3$ ring sharing a Si–O unit. Iso1 ($C_1$) contains a triangular $Si_3$ core with two of the edges bridged by O–Si–O units, thereby forming two $Si_3O_2$ pentagons. This is the first structure found in this work, which presents a segregated silicon trimer core. Iso2 ($C_1$) is also composed of an O-bridged triangular $Si_3$ unit with $Si_3O_2$ and $Si_2O_2$ units fused to it. Iso3 ($C_1$) is composed of two $Si_3O_2$ pentagons sharing a Si atom, forming a nearly linear Si–Si–Si chain.

For this cluster size, the addition of Xe also changes the energetic order slightly. However, all Xe binding energies are similar and relatively small. Consequently, the IR spectra are only little affected. Unfortunately, the comparison between the low-energy $Si_5O_4^+$–Xe isomers with the IRMPD spectrum does not allow for clearly assigning the latter one to a single dominating species.

According to Lu *et al.*,[26] the predicted lowest-energy isomer of neutral $Si_5O_4$ consists of a $Si_2O_2$ and a distorted hexagonal $Si_4O_2$ unit fused under 90° at a common Si atom. This structure corresponds to a cationic structure ($C_{2v}$, not shown here) +0.53 eV higher in energy than iso1. The second most stable neutral isomer (+0.115 eV) corresponds to iso3 (+0.09 eV) and the third (+0.225 eV) to iso1 of the cation, respectively.

### 2. $Si_5O_5^+$(–Xe)

The IR spectra of $Si_5O_5^+$ are compared in the middle panel of Fig. 3. The IRMPD spectrum of $Si_5O_5^+$–Xe is clearly dominated by iso1, and there is convincing agreement between the measured and predicted spectra in the whole spectral range investigated for both intense and weak features. The next two isomers, iso2 and iso3, have a different peak pattern and, in particular, show a prominent peak at about 820 $cm^{-1}$ that is clearly missing in the experimental spectrum. The broad feature ranging from 960 to 1130 $cm^{-1}$ in the recorded spectrum consists of three discernible maxima at 994, 1022, and 1069 $cm^{-1}$. These are attributed to $\sigma_{SiO}$ vibrations of iso1 calculated at 995, 1054, and 1074 $cm^{-1}$, all slightly shifted to the blue of the experimental maxima, with a maximum deviation of 32 $cm^{-1}$ for the middle peak.

Iso1 ($C_{2v}$) consists of a $Si_3O_3$ hexagon and a $Si_3O_2$ pentagon fused under 90° and sharing a tetrahedrally O-coordinated Si atom. This fundamental structural motif of a central tetrahedrally O-coordinated Si atom is found for $Si_3O_4^+$ (iso1), $Si_4O_4^+$ (iso1), and $Si_4O_5^+$ (iso1) and this building block of silicates appears to become important already in these low-oxidized silicon oxide clusters. In iso1-Xe ($C_s$), the Xe atom binds symmetrically to the $Si_2$ unit and lies in the plane of the $Si_3O_3$ hexagon. The Xe–Si bond distance is 3.39 Å and the binding energy is −0.23 eV (−22.24 kJ/mol).

The IRMPD spectrum of pristine $Si_5O_5^+$ reported before[38] is overall quite similar in appearance to the one measured for the Xe-tagged complex, with only modest spectral shifts and some variations in relative intensities. The previous study came to the same structural assignment (iso1), although the contribution of relatively high energy isomers (more than +0.5 eV above iso1) was not ruled out. Our computational search identified many more additional low-energy isomers. However, the good agreement between the IRMPD spectrum of $Si_5O_5^+$–Xe with that predicted for iso1-Xe does not call for major contributions of these higher-energy isomers.

The lowest-energy structure of the cation, iso1, differs from the structure predicted for neutral $Si_5O_5$,[26,66,68] which is similar to iso5 of the cation (+0.51 eV). The neutral structure corresponding to iso1 is predicted to be 0.39 eV higher in energy.[26]

### 3. $Si_5O_6^+$(–Xe)

Unfortunately an IRMPD spectrum of $Si_5O_6^+$–Xe could not be obtained. However, for completeness we report the predictions for the geometries, energies, and IR spectra of this cluster size (right panel of Fig. 3). Iso1 has a structure similar to iso5 of $Si_4O_5^+$ with a Si–O unit added to one of the two $Si_3O_2$ units forming a $Si_2O_2$ rhombus. The geometries of iso2 (+0.03 eV) and iso3 (+0.29 eV) differ only slightly from that of iso1 and are also based on the iso5 structure of $Si_4O_5^+$. Iso4 (+0.31 eV, $C_{2v}$) is composed of two $Si_3O_3$ hexagons featuring a central tetrahedrally coordinated Si atom. This isomer corresponds to the structure that would be formed if an additional O atom were inserted between the $Si_2$ unit of iso1 of $Si_5O_5^+$. Surprisingly, this structure does not represent the predicted lowest energy isomer, in analogy to the formation of $Si_3O_3^+$ iso1 from $Si_3O_2^+$ iso1. The last isomer, iso5 (+0.47 eV, $C_1$), presented here can be described as a combination of two distorted $Si_3O_3$ hexagons fused together at one common Si–O bond with a bridged O on top of one of these two units.

The predicted lowest-energy structure of neutral $Si_5O_6$ clusters[26,65] corresponds to iso4 of the cation, and the lowest energy isomer iso1 of the cations to the third neutral isomer (+1.38 eV).[26]

## IV. CONCLUSIONS

Cluster-size specific vibrational spectra of $Si_nO_m^+$–Xe with n = 3–5 and m = n, n ± 1 in the gas phase have been measured using IRMPD, and structural assignments have been carried out by comparison to results of DFT calculations. The experimental spectra reported here for the stoichiometric $(SiO)_n^+$–Xe clusters support the previous results from Garand *et al.*[38] for bare $(SiO)_n^+$ but represent an improvement in spectral resolution and sensitivity due to the messenger approach and an extension in the spectral range

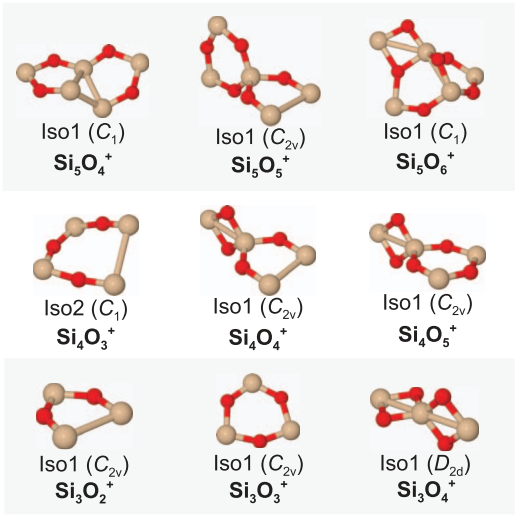


FIG. 4. Structures of the $Si_nO_m^+$ isomers, which could be assigned to the corresponding experimental IRMPD spectra, calculated at the ri-TPSS/def2-TZVP level of theory along with the symmetry group and the electronic state (in parenthesis). Rows show structures with constant numbers of Si atoms (n) and increasing numbers of O atoms. Columns show structures with increasing numbers of SiO units. The central column shows the stoichiometric silicon monoxide cations $(SiO)_{3-5}^+$.

investigated (250–1250 $cm^{-1}$ vs. 500–1250 $cm^{-1}$). For most cases, the IRMPD spectra measured for $Si_nO_m^+$–Xe are assigned to the lowest energy isomer of the bare clusters predicted by DFT calculations or, in cases where Xe changed the energetic ordering, to the lowest energy isomer of the Xe-tagged complexes. Except for $Si_3O_4^+$, where the quality of the experimental spectrum is poor, there is compelling agreement between the experimental and the calculated IR spectrum for the assigned species. The combined spectroscopic and computational approach gives detailed insight into the size and composition dependent structural evolution of small $Si_nO_m^+$(-Xe) clusters. In Fig. 4, we present an overview of the assigned $Si_nO_m^+$ cluster structures, where the Xe is omitted for clarity. These structures show that there is no simple sequential growth mechanism. However, one can clearly identify structural motifs, which serve as building blocks for the low-energy $Si_nO_m^+$ clusters. These include the $Si_2O_2$ rhombus, the $Si_3O_2$ pentagon, and the $Si_3O_3$ hexagon. All of the isomers, apart from iso2 of $Si_4O_3^+$, contain one or more of these building blocks. Another recurring structural element is a central Si atom tetrahedrally coordinated by four O atoms. All of the clusters containing at least four O atoms, except for $Si_5O_4^+$, contain such a structural element. This element often leads to geometries with ring units fused together at an angle of 90°. For many cluster sizes, the most stable cation structure differs from that of the neutral species, indicating that removal of an electron has a drastic impact on the preferred geometry of these small silicon oxide clusters.

In the Xe complexes, the Xe atom binds exclusively to Si atoms, either to a single atom or symmetrically bridging a Si–Si bond. The calculated binding energies vary over a wide range between −0.08 and −1.02 eV (see supplementary material).[71] The Si–Xe bond length varies between 2.71 and 3.49 Å and is correlated with the Si–Xe binding energy. For instance, the bond lengths are very similar in $Si_3O_3^+$–Xe and $Si_4O_5^+$–Xe (2.95 Å), as are the calculated binding energies (−0.38 and −0.37 eV). The bond strength depends on the transfer of electron density from Xe to the (partially) positively charged Si centers. For some cluster sizes, the substantial differences in the Xe binding energies result in a change of the energetic ordering of the isomers in the Xe complexes compared to that of the bare clusters. The overall influence of the Xe binding on the cluster geometries and IR spectra is small, apart from the effects due to the reduction of symmetry, which increases the number of IR active modes.

## ACKNOWLEDGMENTS

This work was supported by the Deutsche Forschungsgemeinschaft (DFG) within the research unit FOR 1282 (DO 729/5, FI 893/4, RE 1509/9). We gratefully acknowledge the support of the "Stichting voor Fundamenteel Onderzoek der Materie" (FOM) in providing beam time of FELIX and we highly appreciate the skillful assistance of the FELIX staff, in particular B. Redlich and A. F. G. van der Meer. The research leading to these results received funding from the European Community's Seventh Framework program (FP7/2007-2013) under Grant Agreement No. 226716.

[1] S. A. Claridge, A. W. Castleman, S. N. Khanna, C. B. Murray, A. Sen, and P. S. Weiss, ACS Nano **3**, 244 (2009).
[2] D. J. Henry, J. Phys. Chem. C **116**, 24814 (2012).
[3] D. Mocatta, G. Cohen, J. Schattner, O. Millo, E. Rabani, and U. Banin, Science **332**, 77 (2011).
[4] Y. Niihori, W. Kurashige, M. Matsuzaki, and Y. Negishi, Nanoscale **5**, 508 (2013).
[5] B. J. Nagare, S. Jaware, D. Habale, and S. Chavan, Comput. Mater. Sci. **68**, 127 (2013).
[6] L. Landt, C. Bostedt, D. Wolter, T. Möller, J. E. P. Dahl, R. M. K. Carlson, B. A. Tkachenko, A. A. Fokin, P. R. Schreiner, A. Kulesza, R. Mitrić, and V. Bonačić-Koutecký, J. Chem. Phys. **132**, 144305 (2010).
[7] M. Vörös, T. Demjén, T. Szilvási, and A. Gali, Phys. Rev. Lett. **108**, 267401 (2012).
[8] T. Iwasa and A. Nakajima, J. Phys. Chem. C **116**, 14071 (2012).
[9] B. Marsen, M. Lonfat, P. Scheier, and K. Sattler, Phys. Rev. B **62**, 6892 (2000).
[10] L. T. Canham, Appl. Phys. Lett. **57**, 1046 (1990).
[11] A. A. Gnidenko and V. G. Zavodinsky, Semiconductors **42**, 800 (2008).
[12] M. A. R. George, M. Savoca, and O. Dopfer, Chem. – Eur. J. **19**, 15315 (2013).
[13] M. Savoca, M. A. R. George, J. Langer, and O. Dopfer, Phys. Chem. Chem. Phys. **15**, 2774 (2013).
[14] M. Savoca, J. Langer, and O. Dopfer, Angew. Chem., Int. Ed. **52**, 1568 (2013).
[15] R. Kumar, Y. Kitoh, K. Shigematsu, and K. Hara, Jpn. J. Appl. Phys., Part 1 **33**, 909 (1994).
[16] T. Schenkel, T. Schlatholter, M. W. Newman, G. A. Machicoane, J. W. McDonald, and A. V. Hamza, J. Chem. Phys. **113**, 2419 (2000).
[17] D. Palagin and K. Reuter, ACS Nano **7**, 1763 (2013).
[18] B. Garrido Fernandez, M. López, C. García, A. Pérez-Rodríguez, J. R. Morante, C. Bonafos, M. Carrada, and A. Claverie, J. Appl. Phys. **91**, 798 (2002).
[19] T. Inokuma, Y. Wakayama, T. Muramoto, R. Aoki, Y. Kurata, and S. Hasegawa, J. Appl. Phys. **83**, 2228 (1998).
[20] T. Shimizu-Iwayama, S. Nakao, and K. Saitoh, Appl. Phys. Lett. **65**, 1814 (1994).
[21] S. F. Li and X. G. Gong, J. Chem. Phys. **122**, 174311 (2005).
[22] A. C. Reber, P. A. Clayborne, J. U. Reveles, S. N. Khanna, A. W. Castleman, Jr., and A. Ali, Nano Lett. **6**, 1190 (2006).
[23] R. Zhang, M. Zhao, and S. Lee, Phys. Rev. Lett. **93**, 095503 (2004).

[24]H. Wang, J. Sun, W. C. Lu, Z. S. Li, C. C. Sun, C. Z. Wang, and K. M. Ho, J. Phys. Chem. C **112**, 7097 (2008).
[25]Q. J. Zang, Z. M. Su, W. C. Lu, C. Z. Wang, and K. M. Ho, J. Phys. Chem. A **110**, 8151 (2006).
[26]W. C. Lu, C. Z. Wang, V. Nguyen, M. W. Schmidt, M. S. Gordon, and K. M. Ho, J. Phys. Chem. A **107**, 6936 (2003).
[27]H.-P. Gail and E. Sedlmayr, Faraday Discuss. **109**, 303 (1998).
[28]S. A. Krasnokutski, G. Rouillé, C. Jäger, F. Huisken, S. Zhukovska, and T. Henning, Astrophys. J. **782**, 15 (2014).
[29]K. D. Gordon, A. N. Witt, and B. C. Friedmann, Astrophys. J. **498**, 522 (1998).
[30]A. N. Witt, K. D. Gordon, and D. G. Furton, Astrophys. J. **501**, L111 (1998).
[31]J. Fan, J. B. Nicholas, J. M. Price, S. D. Colson, and L.-S. Wang, J. Am. Chem. Soc. **117**, 5417 (1995).
[32]L. S. Wang, S. R. Desai, H. Wu, and J. B. Nicholas, Z. Phys. D **40**, 36 (1997).
[33]L.-S. Wang, J. Nicholas, M. Dupuis, H. Wu, and S. Colson, Phys. Rev. Lett. **78**, 4450 (1997).
[34]L.-S. Wang, H. Wu, S. R. Desai, J. Fan, and S. D. Colson, J. Phys. Chem. **100**, 8697 (1996).
[35]J. S. Anderson, J. Chem. Phys. **51**, 4189 (1969).
[36]J. S. Anderson, J. S. Ogden, and M. J. Ricks, Chem. Commun. (London) **1968**, 1585.
[37]J. S. Ogden, Spectrochim. Acta, Part A **33**, 1059 (1977).
[38]E. Garand, D. Goebbert, G. Santambrogio, E. Janssens, P. Lievens, G. Meijer, D. M. Neumark, and K. R. Asmis, Phys. Chem. Chem. Phys. **10**, 1502 (2008).
[39]M. Okumura, L. I. Yeh, J. D. Myers, and Y. T. Lee, J. Chem. Phys. **85**, 2328 (1986).
[40]M. Okumura, L. I. Yeh, and Y. T. Lee, J. Chem. Phys. **83**, 3705 (1985).
[41]M. Savoca, J. Langer, D. J. Harding, O. Dopfer, and A. Fielicke, Chem. Phys. Lett. **557**, 49 (2013).
[42]C. Kerpal, D. J. Harding, A. C. Hermes, G. Meijer, S. R. Mackenzie, and A. Fielicke, J. Phys. Chem. A **117**, 1233 (2013).
[43]K. Mizuse and A. Fujii, Phys. Chem. Chem. Phys. **13**, 7129 (2011).
[44]K. R. Asmis, T. Wende, M. Bruemmer, O. Gause, G. Santambrogio, E. C. Stanca-Kaposta, J. Doebler, A. Niedziela, and J. Sauer, Phys. Chem. Chem. Phys. **14**, 9377 (2012).
[45]R. Gehrke, P. Gruene, A. Fielicke, G. Meijer, and K. Reuter, J. Chem. Phys. **130**, 034306 (2009).
[46]D. Oepts, A. F. G. van der Meer, and P. W. van Amersfoort, Infrared Phys. Technol. **36**, 297 (1995).
[47]A. Fielicke, G. von Helden, and G. Meijer, Eur. Phys. J. D **34**, 83 (2005).
[48]M. Haertelt, J. T. Lyon, P. Claes, J. de Haeck, P. Lievens, and A. Fielicke, J. Chem. Phys. **136**, 064301 (2012).
[49]D. J. Wales, Philos. Trans. R. Soc., A **363**, 357 (2005).
[50]V. Blum, R. Gehrke, F. Hanke, P. Havu, V. Havu, X. Ren, K. Reuter, and M. Scheffler, Comput. Phys. Commun. **180**, 2175 (2009).
[51]J. P. Perdew, K. Burke, and M. Ernzerhof, Phys. Rev. Lett. **77**, 3865 (1996).
[52]D. J. Harding, C. Kerpal, G. Meijer, and A. Fielicke, J. Phys. Chem. Lett. **4**, 892 (2013).
[53]TURBOMOLE V6.3.1, a development of University of Karlsruhe and Forschungszentrum Karlsruhe GmbH, 1989–2007, TURBOMOLE GmbH, since 2007.
[54]J. Perdew, Phys. Rev. B **33**, 8822 (1986).
[55]A. D. Becke, Phys. Rev. A **38**, 3098 (1988).
[56]J. Tao, J. Perdew, V. Staroverov, and G. Scuseria, Phys. Rev. Lett. **91**, 146401 (2003).
[57]D. Rappoport and F. Furche, J. Chem. Phys. **133**, 134105 (2010).
[58]A. Hellweg, C. Hättig, S. Höfener, and W. Klopper, Theor. Chem. Acc. **117**, 587 (2007).
[59]K. Eichkorn, O. Treutler, H. Öhm, M. Häser, and R. Ahlrichs, Chem. Phys. Lett. **240**, 283 (1995).
[60]R. Beer, D. L. Lambert, and C. Sneden, Publ. Astron. Soc. Pac. **86**, 806 (1974).
[61]R. V. Olkhov, S. A. Nizkorodov, and O. Dopfer, Chem. Phys. **239**, 393 (1998).
[62]M. Jadraque, M. Santos, L. Díaz, J. Álvarez-Ruiz, and M. Martín, J. Phys. Chem. A **113**, 10880 (2009).
[63]M. Dupuis and J. B. Nicholas, Mol. Phys. **96**, 549 (1999).
[64]P. V. Avramov, I. Adamovic, K.-M. Ho, C. Z. Wang, W. C. Lu, and M. S. Gordon, J. Phys. Chem. A **109**, 6294 (2005).
[65]A. C. Reber, S. Paranthaman, P. A. Clayborne, S. N. Khanna, and A. W. Castleman, ACS Nano **2**, 1729 (2008).
[66]H.-B. Du, S.-P. Huang, A. de Sarkar, W.-J. Fan, Y. Jia, and R.-Q. Zhang, "Electronic and vibrational properties of stable isomers of $(SiO)_n^{(0,\pm)}$ ($n = 2-7$) clusters," J. Phys. Chem. A (published online 2014).
[67]T. S. Chu, R. Q. Zhang, and H. F. Cheung, J. Phys. Chem. B **105**, 1705 (2001).
[68]S.-X. Hu, J.-G. Yu, and E. Y. Zeng, J. Phys. Chem. A **114**, 10769 (2010).
[69]A. E. Reed, R. B. Weinstock, and F. Weinhold, J. Chem. Phys. **83**, 735 (1985).
[70]J. Chelikowsky, Phys. Rev. B **57**, 3333 (1998).
[71]See supplementary material at http://dx.doi.org/10.1063/1.4894406 for frequencies, structural coordinates, and IR spectra of various isomers of $Si_nO_m^+$(–Xe) clusters.